Computational Study of Bridge-Assisted Intervalence Electron Transfer

Feizhi Ding,[†] Haobin Wang,*[,†] Qin Wu,[‡,§] Troy Van Voorhis,[‡] Shaowei Chen,*[,∥] and Joseph P. Konopelski[∥]

Department of Chemistry and Biochemistry, New Mexico State University, Las Cruces, New Mexico 88003, Department of Chemistry, Massachusetts Institute of Technology, Cambridge, Massachusetts 02139, and Department of Chemistry and Biochemistry, University of California, Santa Cruz, California 95064

Received: December 21, 2009; Revised Manuscript Received: April 19, 2010

Intervalence electron transfer reactions were studied computationally by means of density functional theory and constrained density functional theory (CDFT). Two ferrocene moieties, connected via various bridge structures, were used as model mixed-valence compounds in the computational investigation. Features of the frontier orbitals were analyzed to offer a qualitative account of the intervalence characteristics of the model complexes. The effective electronic coupling between the donor and acceptor sites was calculated using the CDFT method, which provided a quantitative measure of the intervalence electronic communication. The relationship between the bridge linkage and the effectiveness of intervalence transfer was discussed on the basis of the theoretical results and compared to experimental data available in the literature.

Introduction

There are continuous interests in molecular mixed-valence systems due to the effective electronic communication between different sites of the compounds and the resulting unique optoelectronic properties upon photoexcitation.[1−10] In many situations a mixed-valence system consists of a donor, an acceptor, and a bridge unit that connects them. The donor and acceptor sites typically contain a transition metal center that is surrounded by organic ligands. Depending on the nature of the chemical bridge, the optical transitions of the mixed-valence system may exhibit a characteristic metal-to-metal charge-transfer (MMCT) band. Traditionally, mixed-valence systems are classified by the degree of charge delocalization or the extent of interactions (α) between the donor and acceptor sites. According to the criteria proposed by Robin and Day,[11] there are three types of mixed-valence compounds: class I compounds that exhibit little or no interaction ($\alpha \approx 0$), class III compounds with extensive charge delocalization ($\alpha = 0.707$), and class II compounds that fall into the intermediate range ($0 < \alpha < 0.707$). The intervalence electron transfer process in class II and III complexes is often ultrafast, which promotes effective electronic communication and charge delocalization between different molecular moieties within the overall mixed-valence complex. The relatively strong electronic coupling between the donor and acceptor states is primarily determined by two contributing factors: (i) direct overlap of the orbitals of the two metal centers (i.e., through-space interactions) and (ii) metal−ligand−metal overlap that may involve σ or π metal−ligand bonds (i.e., through-bond interactions). When the metal centers are separated by a sufficiently long distance, the contribution from the first factor will be minimal, whereas the second contribution becomes predominant, which may be readily varied by the specific ligand structure and metal−ligand bonding interactions.

Extensive work has been carried out on the synthesis and characterization of various donor−bridge−acceptor mixed-valence systems, particularly with two or more identical molecular moieties (the donor as well as the acceptor) that are linked by a conjugated organic bridge[8−10,12−24] or bound onto metal surfaces by virtue of metal−ligand π bonds.[25,26] When the bridge contains sp^3 carbons, the electronic communication diminishes drastically.[27] Furthermore, as has been predicted by McConnell's superexchange model and also observed experimentally, the effective electronic coupling between the donor and acceptor sites decreases significantly with increasing length of the bridge unit (quantum perturbation theory predicts that the electronic coupling drops exponentially versus the length of the bridge).

In the present study, we carry out a systematic computational study to examine the bridge-assisted intervalence transfer processes for various ferrocene−bridge−ferrocene model systems. The purpose of our work is to investigate the relationship between the property of the bridge linkage and the effective electronic coupling of the overall system. In the next section we will first describe briefly the models and the computational methods employed in our work. Then we will present the results and the detailed analysis on the intervalence coupling/communication. In the conclusion we discuss the implication of our computational study in future experimental studies.

Models and Computational Methods

To study bridge-assisted intervalence electron transfer, we consider a model with two ferrocene (Fc) units connected by different structural linkages. Unless specified otherwise, the total charge of the overall system was set to +1, i.e., with an electron transferred from the donor state (Fe^{2+}) to the acceptor state (Fe^{3+}). Various bridge units were considered, including saturated C−C single bonds, conjugate C═C double bonds, multiple C≡C triple bonds, aromatic rings, and the mixture between some of them. The size of the bridge unit was systematically varied to

* To whom correspondence should be addressed, haobin@nmsu.edu (H.B.W.) and schen@chemistry.ucsc.edu (S.W.C.).
† New Mexico State University.
‡ Massachusetts Institute of Technology.
§ Present address: Center for Functional Nanomaterials, Brookhaven National Laboratory, Upton, NY 11973.
∥ University of California, Santa Cruz.

10.1021/jp912049p
Published on Web 04/29/2010

study the property of the intervalence transfer versus the distance between the donor and the acceptor states.

Two computational approaches were used in this work. The standard density functional theory (DFT) was used to study the equilibrium properties of the mixed-valence complexes as well as the characteristics of the corresponding frontier orbitals. The constrained density functional theory (CDFT)[28−34] was employed to calculate the electronic coupling matrix element (or transfer integral) for the underlying intervalence transfer.[35] The basic idea of the CDFT approach is to impose an external constraint via the method of Lagrange multiplier, i.e., adding an effective potential $V_c w_c(\mathbf{r})$ to the Hamiltonian. The resulting ground-state density satisfies specific density constraints, i.e., $\int w_c(\mathbf{r})\rho_c(\mathbf{r})\, d\mathbf{r} = N_c$, where $w_c(\mathbf{r})$ is the operator that defines the property of interest, e.g., the electronic population, while N_c is the target value. To study the electron transfer process, this constraint is naturally defined as the charge difference (Δq) between the two ferrocenyl groups: $\Delta q = -1$ for the donor state and $\Delta q = +1$ for the acceptor state. For a given constraint, our CDFT method[29,30] uses a direct optimization within the usual self-consistent procedure of DFT to find the minimum energy, the electronic density (or the Kohn−Sham orbitals), and the constrained potential (the Lagrange multiplier V_c). The two different charge constraints then define two (approximate) diabatic states for the donor and the acceptor in the electron transfer model and the resulting two-state Hamiltonian matrix.[35] After appropriate orthogonalization of the two diabatic states (in this work the Löwdin orthogonalization[36,37] was used), the electronic coupling matrix element can be readily evaluated.

The DFT calculations were performed using the quantum chemical program Gaussian 03,[38] whereas the CDFT and electronic coupling calculations were carried out with a modified version of the quantum chemical program NWCHEM.[39] In both simulations the B3LYP hybrid functional, which includes the Becke three-parameter exchange[40] and the Lee, Yang, and Parr correction functionals,[41] were employed. In most calculations the LANL2DZ basis sets[42] were used in the calculation for the transition metal Fe, whereas the 6-31G** basis sets[43] were used for other elements such as C, N, O, and H. Full geometric optimizations were performed in the DFT calculations for most of the systems, and geometric optimizations were performed in the CDFT calculations for some systems. In some calculations the solvent effects were taken into account approximately by the COSMO approach.[44]

Results and Discussion

A picture that is often adopted for long-distance electron transfer is the McConnell's superexchange mechanism.[45] In this model the effective donor−acceptor electronic coupling is determined by the orbital overlaps between all the connecting sites. The role of the bridge linkage is to provide an enhancement of the transfer matrix element (in comparison with the vacuum) instead of actual localized states for sequential electron hopping. In McConnell's original work, perturbation theory was employed to evaluate the effective electronic coupling matrix element. Although this may break down for a strongly coupled mixed-valence system, many qualitative arguments are still expected to be valid. For example, delocalization of the frontier orbitals for the overall system is necessary to facilitate long-distance electron transfer since it is the direct consequence of the orbital overlaps between different sites. This favors a bridge structure with conjugate π bonds. It is expected that the length of the bridge linkage as well as other properties may also affect the electronic coupling between the donor and the acceptor sites. Below we will give a detailed account of all these effects.

TABLE 1: Electronic Coupling (H_{ab}) for the Fc−CH═CH−Fc$^+$ System

	H_{ab} (kcal/mol)	
basis	gas phase	CH_2Cl_2 solution (COSMO)
LanL2DZ	3.47	1.96
mixed[a]	3.22	1.90
6-31G**	3.53	2.13
6-311G**	3.46	2.04

[a] Mixed basis: 6-31G** for C and H atoms; LanL2DZ pseudopotential for Fe atoms.

Simple Bridge Linkages. To examine the dependence of the theoretical results on the different basis sets used in the calculations we first carried out DFT calculations for the biferrocenyl monocation, Fc−CH═CH−Fc$^+$. Four different sets of basis functions were employed: (a) the LANL2DZ basis set for all elements; (b) a mixed basis set with the LANL2DZ basis function for Fe and 6-31G** series of basis functions for C and H; (c) the 6-31G** basis set for all elements; and (d) the 6-311G** basis set for all elements. The qualitative features of the frontier orbitals are the same for all the basis sets employed, which suggests that the physical observables of interest in this paper are not very sensitive to the basis functions employed in the calculation. A more quantitative comparison is given in Table 1, where the electronic coupling (H_{ab}) between the donor and acceptor Fc sites is evaluated using the CDFT approach with different basis functions. The calculated values are in very good agreement with each other both in gas phase and in dichloromethane (CH_2Cl_2) solutions. This confirms that the use of different basis functions makes negligible differences for the properties discussed in this paper. Therefore, in all the results presented below, we will use the mixed basis set where the LANL2DZ basis functions are used for transition metals such as Fe and the 6-31G** basis functions for other elements.

Figure 1 shows the DFT calculated frontier orbitals for nine mixed-valence model systems (I) Fc−Fc$^+$, (II) Fc−CH_2−CH_2−Fc$^+$, (III) Fc−CH═CH−Fc$^+$, (IV) Fc−C≡C−Fc$^+$, (V) Fc−1,2,3-triazole−Fc$^+$ (in the following we denote 1,2,3-triazole simply as "triazole"), (VI) Fc−benzene−Fc$^+$, (VII) Fc−pyrazine−Fc$^+$, (VIII) Fc−pyridine−Fc$^+$, and (IX) Fc−pyrimidine−Fc$^+$. Full geometry optimizations were carried out for all the structures. The highest occupied molecular orbitals (HOMOs) are shown in Figure 1a and the lowest unoccupied molecular orbitals (LUMOs) in Figure 1b. It can be seen that the frontier orbitals of the model systems display varied degrees of delocalization across the entire complexes. The extent of the delocalization depends rather sensitively on the level of conjugation of the bridge group. For complex II, where the bridge structure is a saturated C−C single bond, the frontier orbitals exhibit little contribution from the bridge. For complex V the contribution from the nonaromatic bridge is also small. In sharp contrast, for other complexes with conjugated bridges, apparent delocalization can be readily seen across the entire molecules. For some of the model systems the optimized geometries do not possess C_i symmetry; hence the two ferrocenyl groups are not energetically degenerate. This diminishes delocalization of the MOs across the whole system. On the other hand, for systems where the two ferrocenyl groups have approximately the same energy (e.g., VI) the frontier orbitals delocalize across the entire Fc−bridge−Fc structure.

The delocalization of the frontier orbitals is indicative of an effective electronic coupling between the donor/acceptor states via the bridge moiety. From the point of view of diabatic (resonant states) to adiabatic (molecular eigenstates) transforma-

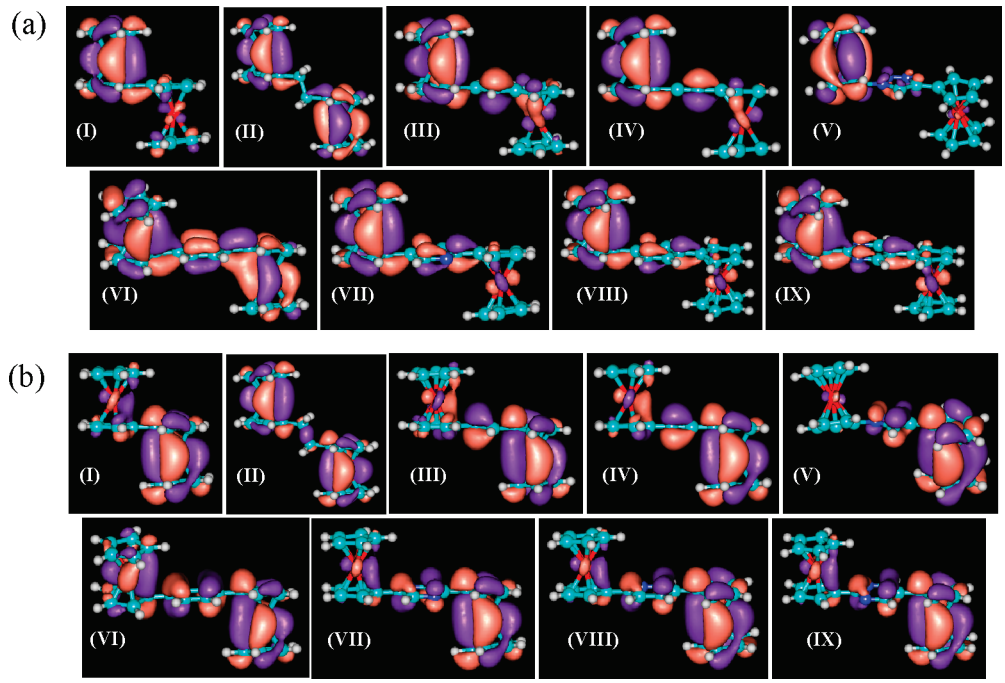

Figure 1. (a) HOMO and (b) LUMO topological diagrams for (I) Fc—Fc^+, (II) Fc—CH_2—CH_2—Fc^+, (III) Fc—CH═CH—Fc^+, (IV) Fc—C≡C—Fc^+, (V) Fc−triazole−Fc^+, (VI) Fc−benzene−Fc^+, (VII) Fc−pyrazine−Fc^+, (VIII) Fc−pyridine−Fc^+, and (IX) Fc−pyrimidine−Fc^+.

TABLE 2: H_{ab} for Different Fc—bridge—Fc^+ Systems

compound	H_{ab} (kcal/mol)	
	gas phase	CH_2Cl_2 solution (COSMO)
(I) Fc—Fc^+	3.26	2.03
(II) Fc—CH_2—CH_2—Fc^+	0.88	0.41
(III) Fc—CH═CH—Fc^+	3.22	1.90
(IV) Fc—C≡C—Fc^+	2.82	1.69
(V) Fc−triazole−Fc^+	1.82	0.56
(VI) Fc−benzene−Fc^+	1.99	1.08
(VII) Fc−pyrazine−Fc^+	1.78	0.94
(VIII) Fc−pyridine−Fc^+	1.85	0.99
(IX) Fc−pyrimidine−Fc^+	1.69	0.91

tion, these frontier orbitals are linear combinations of the HOMO of the donor site and the LUMOs of the acceptor site and the bridge linkage. The resulting electron transfer thus proceeds via the superexchange mechanism, in which the virtual bridge state provides an effective increase in the coupling element for electron transfer. Different from other model systems, the bridge structure in complex II does not possess any conjugated π bond and is thus more localized. The bridge in complex V contains π bonds but there is a break in conjugation. Thus, the electronic couplings for the intervalence transfer is expected to be weaker for these two model systems than that of the rest of the series.

It should be noted that the conventional DFT method often tends to exaggerate the delocalization of the frontier orbitals. Thus, while there is some interpretive value in the pictures of the frontier orbitals as exemplified in Figure 1, caution must be taken in relating them to real situations. To have a more quantitative description of the bridge-assisted intervalence transfer, we have applied the CDFT approach to evaluate the electronic couplings (H_{ab}) for all the model systems in Figure 1. The calculated H_{ab} values (in kcal/mol) are listed in Table 2 for the Fc−bridge−Fc^+ systems in both gas phase and in CH_2Cl_2 solution (the latter was modeled by the COSMO approach). The DFT optimized geometries were used in all the CDFT calculations. Consistent with the frontier orbital pictures in Figure 1, the electronic couplings are quite large for all compounds except for II the Fc—CH_2—CH_2—Fc^+ system where no π bond is present in the bridge unit and for V the Fc—triazole—Fc^+ system where there is a break of conjugation in the bridge linkage.

A more accurate classification can be made according to the calculated H_{ab} values in CH_2Cl_2 solution. Three groups of compounds can be identified. The first group contains the bare diferrocenyl monocation (complex I) and the compounds with short conjugated bridge structures such as —CH═CH— (complex III) and —C≡C— (complex IV). For these complexes H_{ab} is all greater than 1 kcal/mol, resulting in significant intervalence electronic communication. From experimental voltammetric measurements, complexes Fc—Fc^+, Fc—CH═CH—Fc^+, and Fc—C≡C—Fc^+ all exhibit two distinct oxidation processes[22,46,47] in CH_2Cl_2 ($\Delta E_{1/2} = 350$ mV[46] for Fc—Fc^+, $\Delta E_{1/2} = 160$ mV[22,47] for Fc—CH═CH—Fc^+, $\Delta E_{1/2} = 140$ mV[46] for Fc—C≡C—Fc^+), and all have been classified as class II mixed-valence ions. Thus, our calculations are consistent with the experiment.

The second group contains compounds with large aromatic ring bridge units, such as complexes VI to IX. The calculated H_{ab} is ~1 kcal/mol for these compounds in CH_2Cl_2, making them along the borderline between class I and class II compounds in Robin−Day classification. The relatively weak electronic communication may thus be difficult to resolve experimentally. For instance, in voltammetric measurements one may observe one single pair of broad voltammetric waves, instead of two pairs of well-defined voltammetric peaks as manifested with biferrocene (complex I). Indeed, such electrochemical responses are typical for aromatic ring-bridged biferrocene derivatives, as found in previous experimental measurements.[10]

The third group includes compounds II Fc—CH_2—CH_2—Fc^+ and V Fc−triazole−Fc^+. The calculated H_{ab} values for these two complexes are substantially smaller than the others listed in Table 2. For compound II, $H_{ab} = 0.37$ kcal/mol is the smallest among the series, indicating that the saturated —CH_2—CH_2— bridge unit is not effective to induce electronic communication despite its short length. The nonaromatic 1,2,3-triazole bridge in compound V fares slightly better, with $H_{ab} = 0.56$ kcal/mol; yet the extent of electronic communication is still quite low.

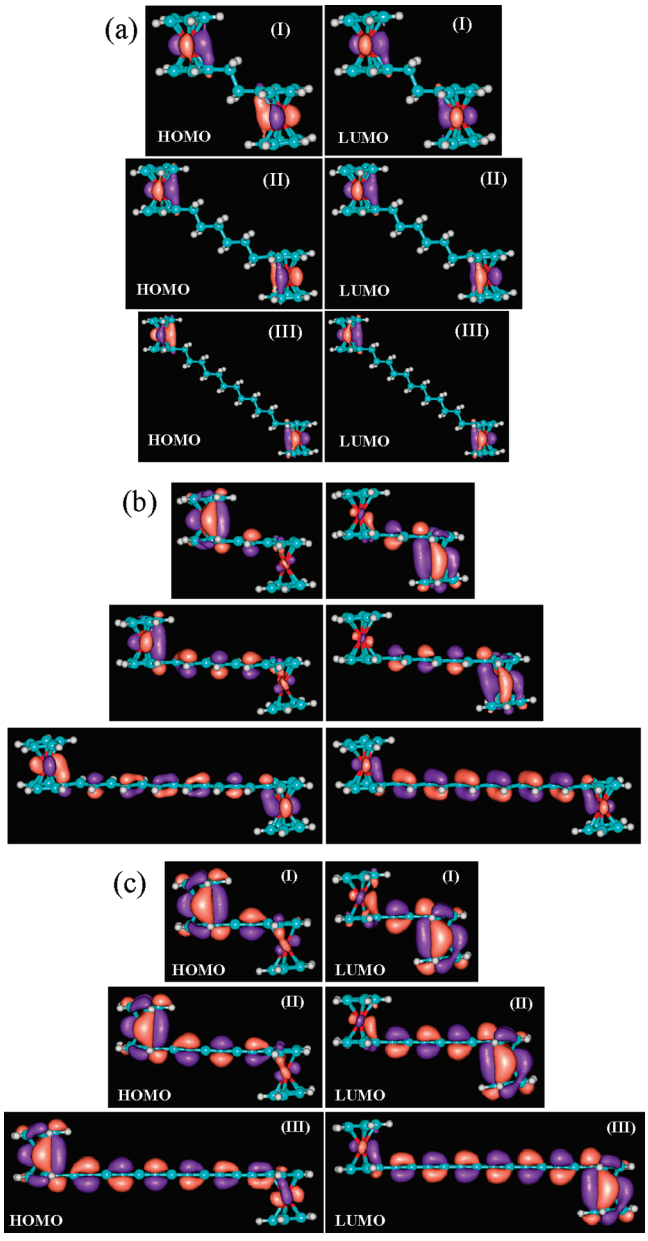

Figure 2. (a) HOMO/LUMO topological diagrams for (I) Fc—CH_2—CH_2—Fc^+, (II) Fc—$(CH_2—CH_2)_3$—Fc^+, and (III) Fc—$(CH_2—CH_2)_6$—Fc^+. (b) HOMO/LUMO topological diagrams for (I) Fc—CH═CH—Fc^+, (II) Fc—$(CH═CH)_3$—Fc^+, and (III) Fc—$(CH═CH)_6$—Fc^+. (c) HOMO/LUMO topological diagrams for (I) Fc—C≡C—Fc^+, (II) Fc—$(C≡C)_3$—Fc^+, and (III) Fc—$(C≡C)_6$—Fc^+.

Thus, it is highly likely that these two compounds belong to class I in Robin−Day classification. In fact, experimentally, electrochemical measurements of complex II exhibited only one pair of voltammetric waves,[8] consistent with the computational results.

Dependence on the Length of the Bridge Structure. Figure 2 shows the DFT calculated frontier orbitals for three types of model systems, (a) Fc-$(CH_2—CH_2)_n$—Fc^+, (b) Fc—$(CH═CH)_n$—Fc^+, and (c) Fc—$(C≡C)_n$—Fc^+, where n is the number of the repetitive bridge structural units. For the saturated bridge structure (Figure 2a), the frontier orbitals are mainly localized in the two ferrocenyl groups. This indicates little overlap between the donor/acceptor Fc states and the bridge states. As a result, the electronic couplings between the two ferrocenyl groups are expected to be small when n becomes large due to the lack of through-bond communication. This is not surprising,

TABLE 3: Dependence of H_{ab} on the Length of the Bridge Unit for Different Fc−bridge−Fc^+ Systems

	H_{ab} (kcal/mol)	
Fc−bridge−Fc^+	gas phase	CH_2Cl_2 solution (COSMO)
	$(C—C)_n$	
Fc—CH_2—CH_2—Fc^+	0.79	0.37
Fc—$(CH_2—CH_2)_3$—Fc^+	0.15	0.04
Fc—$(CH_2—CH_2)_6$—Fc^+	0.03	0.002
	$(C═C)_n$	
Fc—CH═CH—Fc^+	3.22	1.90
Fc—$(CH═CH)_3$—Fc^+	3.42	1.76
Fc—$(CH═CH)_6$—Fc^+	1.02	0.61
	$(C≡C)_n$	
Fc—C≡C—Fc^+	2.82	1.69
Fc—$(C≡C)_3$—Fc^+	2.00	0.97
Fc—$(C≡C)_6$—Fc^+	1.39	0.51

considering the small H_{ab} value even for Fc—CH_2—CH_2—Fc^+ with the shortest bridge (Table 2). In contrast, for a conjugated bridge structure (Figure 2b,c), the frontier orbitals display delocalization characteristics over the entire system. The bridge states will thus effectively participate in the overall intervalence transfer through the superexchange mechanism.

An important point to note is that in Figure 2a the frontier orbitals split over both Fc centers, which is unphysical for such a long saturated bridge. This illustrates that the self-interaction error in DFT may cause incorrect predictions for the ground state properties. A more quantitative study is provided by the CDFT calculations, which are summarized in Table 3. It can be seen that the electronic communication is quite weak for the bridge structure with saturated C−C bonds, suggesting that the DFT frontier orbitals in Figure 2a have the wrong behavior.

For the three types of bridge structures listed in Table 3 the value of H_{ab} in general decreases with increasing bridge length (n). This is consistent with the common qualitative behavior for long-range electron transfer. The trend can be more clearly seen for the H_{ab} values obtained in the CH_2Cl_2 solution (using the COSMO approach). The theoretical findings are consistent with the experiments. For example, based on the experimental results,[46,48,49] the strength of electron communication between the ferrocenyl groups in Fc—$(C≡C)_n$—Fc systems was found to decrease sharply with increasing $(C≡C)_n$ chain length. Fc—C≡C—Fc has a significant experimental splitting of the voltammetric peaks ($\Delta E_{1/2}$ = 140 mV) and has been identified as a typical class II mixed-valence compound in the Robin−Day classification.[46] At n = 3, two closely spaced redox peaks ($\Delta E_{1/2}$ = 60 mV) were observed in cyclic voltammetric measurement,[48] indicating a borderline behavior between class I and class II characteristics. At n = 6, only a single oxidation process was observed,[49] signifying a further diminishment of the electronic coupling. In the previous section we have proposed a scheme to approximately classify the three types of mixed-valence compounds based on the calculated H_{ab} values. According to this classification our CDFT results in Table 3 are in good agreement with these experimental findings for the Fc—$(C≡C)_n$—Fc systems summarized above.

It should be noted that, due to the following reasons, the decrease of H_{ab} may not necessarily follow the exponential decay law derived for the long-distance superexchange electron transfer model. First, the derivation of McConnell's superexchange theory is based on the quantum perturbation theory, which may not be valid for intervalence transfer where strong electronic coupling is present. Second, McConnell's model assumes identical bridge energy levels. If there is some disorder in the

bridge, it will disrupt the exponential decay. Third, if there is true delocalization across the bridge, then the coupling does not have to decay at all.

Table 3 also reveals that for the same number of bridge units (n) the corresponding H_{ab} values are much larger for the conjugated bridges, as depicted in parts b and c of Figure 2, than for the bridges with saturated C−C bonds in Figure 2a, especially when n is large. This suggests that a certain degree of conjugation is needed in order to facilitate effective long-distance electron transfer, which will be further illustrated in later discussion. From the calculated H_{ab} in Table 3, one may conclude that Fc−$(CH_2-CH_2)_n$−Fc^+ compounds belong to class I Robin−Day complex (weak electronic communication); Fc−$(CH=CH)_n$−Fc^+ belongs to class II complex (intermediate electronic communication) even for $n = 3$; whereas Fc−$(C\equiv C)_n$−Fc^+ belongs to class II for $n < 3$ and shows borderline class I/II characteristics at $n = 3$.

Hybrid Bridge Linkage. In practice more flexible bridge linkage may be needed for the purpose of designing effective synthetic routes or enhancing certain physical/chemical properties of the overall mixed-valence complex. In these situations a hybrid bridge linkage may be a more preferable choice. Figure 3 shows the HOMO/LUMO diagrams for varied biferrocenyl derivatives with eight hybrid bridge structures: (I) Fc−CH=CH−C≡C−CH=CH−Fc^+, (II) Fc−CH=CH−benzene−CH=CH−Fc^+, (III) Fc−CH=CH−triazole−CH=CH=Fc^+, (IV) Fc=C≡C=triazole=C≡C=Fc^+, (V) Fc=benzene=triazole=Fc^+, (VI) Fc=benzene=pyrazine=Fc^+, (VII) Fc=CH_2=CH=CH=CH=CH=CH_2=Fc^+, and (VIII) Fc=CH_2=CH_2=CH=CH=CH_2=CH_2=Fc^+. In these, the bridge structures contain two different unsaturated π-bond units, or a mixture of π-bonds and saturated C−C σ-bonds. Combining both the HOMO and LUMO diagrams, the frontier orbitals in complexes I−VI display rather extensive delocalization characteristics, indicating bridge-assisted intervalence transfer. In contrast, the frontier orbitals for complexes VII and VIII are mainly localized in the ferrocenyl groups. This suggests that the corresponding linker is not effective in assisting long-distance electron transfer with the incorporation of sp^3 carbon spacers.

These findings are largely corroborated in the CDFT calculations for the electronic coupling, as listed in Table 4. Specifically, complexes I and II exhibit the largest H_{ab} values (both in gas phase and in CH_2Cl_2 solution) among the series due to the effective conjugation in the bridge structure and the relatively short length of the bridge, whereas the H_{ab} values for complexes VII and VIII are the smallest because of the saturated C−C single bonds in the bridge. The combination of a nonaromatic triazole ring with other conjugated structural units, as shown in complexes III, IV, and V, leads to intermediate H_{ab} values. Interestingly, a comparable H_{ab} was also observed with complex VI. This is likely caused by the relatively poor π-orbital overlaps between the two conjugated rings since they are not on the same plane and has a dihedral angle of 27.5°.

Comparison with H_{ab} Values Obtained from Other Approximate Approaches. Prior to the availability of the CDFT method, approximations are often used to extract H_{ab} from the standard DFT calculations. These approaches are mainly based on the transformation from diabatic to adiabatic representation within a two-state model (Figure 4) and the associated relation obtained between the adiabatic energy gap and the diabatic electronic coupling.[50−53] The most straightforward approach employs Koopman's theorem,[50,51] where the value of H_{ab} is simply approximated as one-half of the energy gap between the highest occupied molecular orbital (HOMO) and the lowest unoccupied molecular orbital (LUMO). Table 5 lists the H_{ab} values obtained from such an approximation. Compared with the values from the CDFT calculations (last column), the H_{ab} values extracted from this approach are much larger. This discrepancy is expected and can be attributed to the self-interaction error present in approximate density functionals, which tends to overstabilize the delocalized state and artificially enhance the coupling. It has been previously shown that CDFT

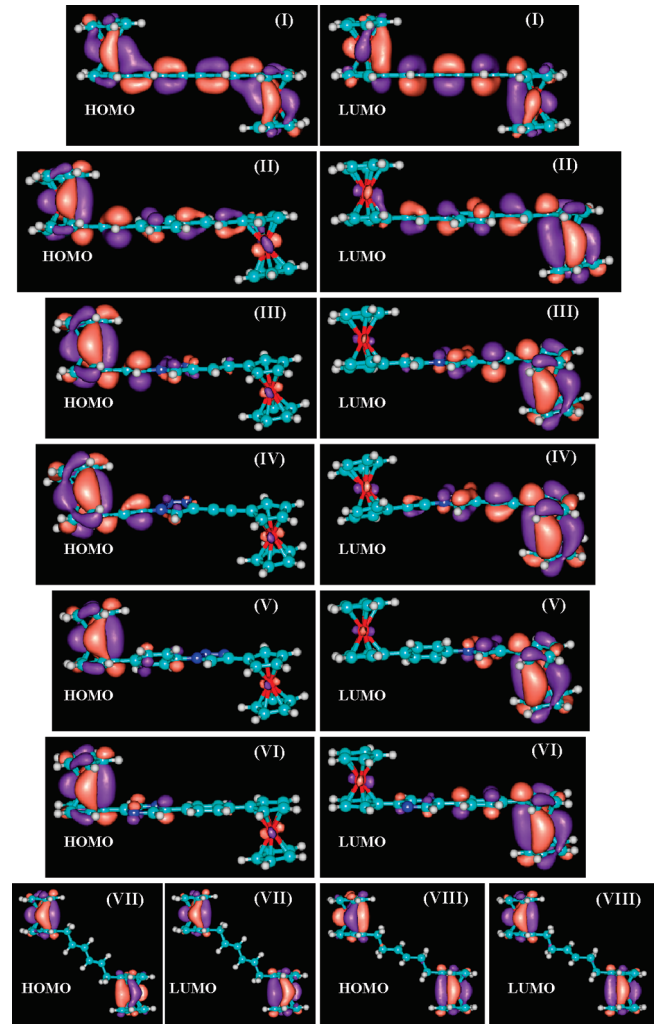

Figure 3. HOMO/LUMO topological diagrams for complexes with hybrid bridge structures: (I) Fc−CH=CH−C≡C−CH=CH−Fc^+, (II) Fc−CH=CH−benzene−CH=CH−Fc^+, (III) Fc−CH=CH−triazole−CH=CH−Fc^+, (IV) Fc−C≡C−triazole−C≡C−Fc^+, (V) Fc−benzene−triazole−Fc^+, (VI) Fc−benzene−pyrazine−Fc^+, (VII) Fc−CH_2−CH=CH−CH=CH−CH_2−Fc^+, and (VIII) Fc−CH_2−CH_2−CH=CH−CH_2−CH_2−Fc^+.

TABLE 4: H_{ab} for the Fc−bridge−Fc Systems with Hybrid Bridge Linkage

compound	H_{ab} (kcal/mol) gas phase	H_{ab} (kcal/mol) COSMO
(I) Fc−CH=CH−C≡C−CH=CH−Fc^+	2.87	1.45
(II) Fc−CH=CH−benzene−CH=CH−Fc^+	2.11	0.91
(III) FcCH=CH−triazole−CH=CH−Fc^+	1.43	0.42
(IV) Fc−C≡C−triazole−C≡C−Fc^+	0.94	0.25
(V) Fc−benzene−triazole−Fc^+	0.63	0.21
(VI) Fc−benzene−pyrazine−Fc^+	1.22	0.49
(VII) Fc−CH_2−CH=CH−CH=CH−CH_2−Fc^+	0.10	0.03
(VIII) Fc−CH_2−CH_2−CH=CH−CH_2−CH_2−Fc^+	0.04	0.01

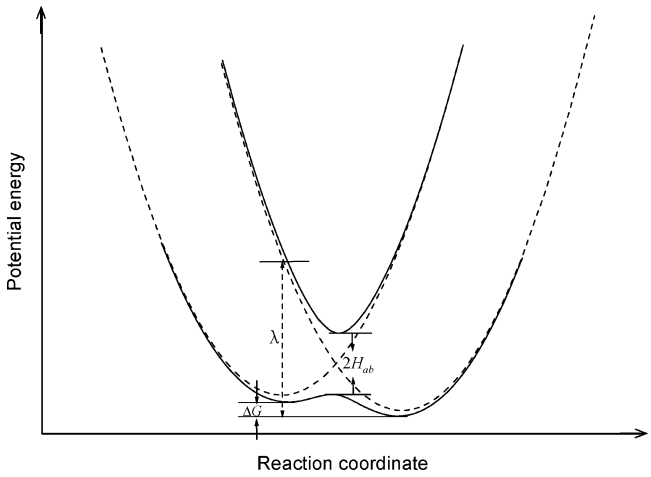

Figure 4. Potential energy curves of one electron transfer reaction in both diabatic representation (dashed lines) and adiabatic representation (solid lines). H_{ab} is the electronic coupling matrix element. λ is the reorganization energy.

gives reliable couplings precisely because it is immune to these systematic errors.[35] We thus conclude that extracting the electronic coupling solely from the DFT results (using Koopman's theorem) is not a practical approach for these systems.

Strictly speaking, the above DFT/Koopman's theorem approach is limited to a symmetric geometry where the donor and the acceptor states have the same energy, which is only approximately satisfied for most of the compounds considered in this paper. With the availability of the CDFT method, it is also in principle possible to extract the value of H_{ab} from the energy differences between the diabatic states obtained from the CDFT calculations and the adiabatic ground state obtained from the standard unconstrained DFT calculations. If the diabatic states are assumed to be approximately orthogonal to each other, the H_{ab} can be estimated as[35]

$$|H_{ab}| = \sqrt{(E - E_D)(E - E_A)} \quad (1)$$

where E_D and E_A are the diabatic state energies for donor and acceptor, respectively, and E represents the ground state energy obtained from the unconstrained DFT. More generally, if we include the overlap S between the two diabatic states and carry out Löwdin orthogonalization, H_{ab} can be expressed by

$$|H_{ab}| = \frac{\sqrt{(E - E_D)(E - E_A)} - S\dfrac{(E - E_D) + (E - E_A)}{2}}{1 - S^2} \quad (2)$$

Absolute values of H_{ab} obtained from eq 1 and eq 2 are collected in Table 5. Once again, due to a much increased self-interaction error for systems with fractional charges, such as the mixed-valence systems considered in this paper, the DFT energy is typically much too low and results in a large overestimation of H_{ab}.[35] As we can see from the table, both eq 1 and eq 2 predict couplings that are quite close to Koopman's theorem—the three methods contain essentially the same incorrect chemistry. We thus find that all three alternative approaches are unreliable and only CDFT provides a qualitatively correct description of the intervalence transfer.

Sensitivity of H_{ab} to the Variation of Nuclear Geometries. In a diabatic representation the nonadiabatic electronic coupling, H_{ab}, often varies slowly with respect to the nuclear coordinates. Thus, many electron transfer theories invoke the Condon approximation where H_{ab} is assumed to be a constant along the reaction coordinate (a collective coordinate of all the nuclear degrees of freedom) and its value is one-half of the adiabatic energy splitting at the crossing point of the diabatic potential energy curves (Figure 4). This approximation usually holds in the regime that is most relevant to the electron transfer process: from the minima of diabatic states to the crossing point, as well as nuclear geometries whose energies are reasonably close to these important configurations (e.g., within several kcal/mol). The Condon approximation will eventually break down for nuclear structures with energies much higher, but these are not relevant to the physical process of electron transfer.

Since the major advantage of the CDFT approach is to find the (approximate) diabatic states, it is worthwhile to investigate the validity of the Condon approximation, i.e., the sensitivity of H_{ab} to the variation of the nuclear geometries. For this purpose we consider the following representative examples for a few Fc−bridge−Fc systems: (1) the unoptimized geometries with energies at least several kcal/mol higher than those of the optimized geometries; (2) the optimized geometries from the standard unconstrained DFT calculation (Ci symmetry is also included for symmetric molecules); and (3) the optimized charge-localized geometries obtained from the CDFT calculations, which were obtained by invoking the constraint that one ferrocene group has one more electron than the other and performing the geometry optimization under this constraint. Table 6 lists the corresponding gas-phase and solution-phase H_{ab} values for several representative molecules at different geometries. It is obvious that all the H_{ab} values exhibit quite weak dependence on the nuclear geometries. This suggests that the diabatic representation that the CDFT calculation gives is rather robust. The thus obtained electronic coupling varies slowly with the nuclear configurations and can be approximated as a constant for the purpose of describing the electron transfer reaction and electronic communication between the diabatic states. As a result, the coupling H_{ab} only needs to be evaluated at some representative nuclear configurations.

Conclusion

In this study both DFT and CDFT methods were employed to study intervalence transfer in the Fc−bridge−Fc model system. The DFT method was good at providing a qualitative description of the delocalization characteristics in frontier orbitals that are typical in mixed-valence systems. It was, however, not capable of predicting the strength of electronic communication and thus could not distinguish class I, II, or III Robin−Day complexes. Furthermore, the self-interaction error that exists in most of the functionals made the DFT method sometimes unreliable because of exaggeration of the extent of electron delocalization.

In contrast, the CDFT method provided a more quantitative description of the intervalence transfer by calculating the electronic coupling between the electron donor and acceptor states. This offers a direct measure of the level of electronic communication. Thus, a practical means of classifying the compounds might be developed by gauging the computational results with the experimental observations. A good example presented in this paper is that for compounds with calculated $H_{ab} \sim 1$ kcal/mol in CH_2Cl_2 their voltammetric response was found along the borderline of class I/II complexes in Robin−Day

TABLE 5: Comparison of H_{ab} Values Obtained from HOMO−LUMO Gap, eq 1, eq 2, and CDFT Calculations for the Fc−bridge−Fc Systems

compound	H_{ab} from HOMO−LUMO gap	H_{ab} from eq 1	H_{ab} from eq 2	H_{ab} from CDFT
Fc−Fc^+	16.6	6.0	6.8	3.26
Fc−CH_2−CH_2−Fc^+	5.5	2.4	2.4	0.88
Fc−CH=CH−Fc^+	14.4	12.6	13.8	3.22
Fc−C≡C−Fc^+	12.9	11.6	12.5	2.82
Fc−triazole−Fc^+	14.2	12.7	13.7	1.82
Fc−benzene−Fc^+	12.3	8.7	9.1	1.99
Fc−pyrazine−Fc^+	14.1	5.0	5.3	1.78
Fc−pyridine−Fc^+	13.4	9.2	9.6	1.85
Fc−pyrimidine−Fc^+	11.8	4.0	4.2	1.69
Fc−$(CH_2$−$CH_2)_3$−Fc^+	2.8	13.1	13.3	0.15
Fc−$(CH_2$−$CH_2)_6$−Fc^+	1.7	13.9	13.9	0.03
Fc−$(CH$=$CH)_3$−Fc^+	13.6	20.2	18.9	3.42
Fc−$(CH$=$CH)_6$−Fc^+	14.2	19.4	21.5	1.02
Fc−$(C$≡$C)_3$−Fc^+	14.4	7.2	7.6	2.00
Fc−$(C$≡$C)_6$−Fc^+	8.8	11.7	12.1	1.39
Fc−CH=CH−C≡C−CH=CH−Fc^+	11.6	12.6	13.5	2.87
Fc−CH=CH−benzene−CH=CH−Fc^+	12.1	12.1	12.8	2.11
Fc−CH=CH−triazole−CH=CH−Fc^+	9.9	11.3	11.8	1.43
Fc−C≡C−triazole−C≡C−Fc^+	7.4	9.8	10.1	0.94
Fc−benzene−triazole−Fc^+	6.3	2.9	3.0	0.63
Fc−benzene−pyrazine−Fc^+	8.6	9.6	9.8	1.22
Fc−CH_2−CH=CH−CH=CH−CH_2−Fc^+	2.8	5.6	5.6	0.10
Fc−CH_2−CH_2−CH=CH−CH_2−CH_2−Fc^+	2.6	6.1	6.1	0.04

TABLE 6: Structural Dependence of H_{ab}[a]

			H_{ab} (kcal/mol)	
compound	geometry	relative energy (kcal/mol)	gas phase	CH_2Cl_2 solution (COSMO)
Fc−CH_2−CH_2−Fc^+	unoptimized geometry 1	5.5	0.79	0.37
	DFT optimized (*Ci* symmetry)	1.6	0.69	0.32
	DFT optimized (no symmetry)	0	0.88	0.41
	CDFT optimized (donor)	1.4	0.60	0.29
Fc−Fc^+	unoptimized geometry 1	36.7	3.30	2.20
	DFT optimized (*Ci* symmetry)	0.01	3.23	2.17
	DFT optimized (no symmetry)	0	3.26	2.03
	CDFT optimized (donor)	7.5	2.56	1.69
Fc−CH=CH−Fc^+	unoptimized geometry 1	13.3	1.58	0.81
	unoptimized geometry 2	5.5	2.01	1.06
	DFT optimized (*Ci* symmetry)	0.9	2.38	1.39
	DFT optimized (no symmetry)	0	3.22	1.90
	CDFT optimized (donor)	1.0	2.34	1.38
	CDFT optimized (acceptor)	0.9	2.48	1.47
Fc−benzene−Fc^+	unoptimized geometry 1	3.8	1.79	0.96
	unoptimized geometry 2	2.8	1.89	1.03
	DFT optimized (*Ci* symmetry)	1.0	2.09	1.15
	DFT optimized (no symmetry)	0	1.99	1.08
	CDFT optimized (donor)	0.6	1.73	0.90
	CDFT optimized (acceptor)	0.6	1.73	0.93
Fc−pyridine−Fc^+	DFT optimized (no symmetry)	0	1.85	0.99
	CDFT optimized (donor)	3.7	1.24	0.65
	CDFT optimized (acceptor)	3.1	1.32	0.70
Fc−$(CH$=$CH)_3$−Fc^+	unoptimized geometry 1	7.8	3.86	1.81
	DFT optimized (*Ci* symmetry)	0.1	3.68	1.63
	DFT optimized (no symmetry)	0	3.42	1.76
	CDFT optimized (donor)	1.4	2.27	0.76
Fc−benzene−pyrazine−Fc^+	unoptimized geometry 1	4.2	1.15	0.46
	DFT optimized (no symmetry)	0	1.22	0.49
	CDFT optimized (donor)	0.6	0.90	0.36
	CDFT optimized (acceptor)	1.7	0.89	0.36

[a] For each molecule, the energy of DFT optimized geometry (with C_1 symmetry) is set to be the reference.

classification. On the basis of this result, the intervalence characteristic of unknown compounds might be predicted from CDFT calculations. That is, CDFT calculation may be a rather effective way in experimental design and interpretation in the study of intervalence transfer with novel compounds and structures.

Acknowledgment. This work was supported by a CRC grant from the National Science Foundation (CHE-0832605, S.W.C., H.B.W., and J.P.K). T.V.V. gratefully acknowledges funding from an NSF CAREER award (CHE-0547877) and a David and Lucille Packard Fellowship. The work also used resources of the National Energy Research Scientific Computing Center,

which is supported by the Office of Science of the U.S. Department of Energy under Contract No. DE-AC02-05CH11231.

References and Notes

(1) Hush, N. S. *Coord. Chem. Rev.* **1985**, *64*, 135–157.
(2) Prassides, K. *Mixed valency systems: applications in chemistry, physics, and biology*; North Atlantic Treaty Organization. Scientific Affairs Division; Kluwer Academic Publishers: Dordrecht and Boston, 1991.
(3) Crutchley, R. J. *Adv. Inorg. Chem.* **1994**, *41*, 273.
(4) Astruc, D. *Electron transfer and radical processes in transition-metal chemistry*; VCH: New York, 1995.
(5) Ward, M. D. *Chem. Soc. Rev.* **1995**, *24*, 121–134.
(6) Allen, G. C.; Hush, N. S. In *Progress in Inorganic Chemistry*; Cotton, F. A., Ed.; Wiley: New York, 2007; pp 357−389.
(7) Ceccon, A.; Santi, S.; Orian, L.; Bisello, A. *Coord. Chem. Rev.* **2004**, *248*, 683–724.
(8) Shu, P.; Bechgaard, K.; Cowan, D. O. *J. Org. Chem.* **1976**, *41*, 1849–1852.
(9) Engtrakul, C.; Sita, L. R. *Nano Lett.* **2001**, *1*, 541–549.
(10) Low, P. J.; Roberts, R. L.; Cordiner, R. L.; Hartl, F. *J. Solid State Electrochem.* **2005**, *9*, 717–731.
(11) Robin, M. B.; Day, P. *Adv. Inorg. Chem. Radiochem.* **1967**, *10*, 247–422.
(12) Cowan, D. O.; Levanda, C.; Park, J.; Kaufman, F. *Acc. Chem. Res.* **1973**, *6*, 1–7.
(13) Day, P.; Hush, N. S.; Clark, R. J. H. *Philos. Trans. R. Soc. London, Ser. A* **2008**, *366*, 5–14.
(14) Gamelin, D. R.; Bominaar, E. L.; Mathoniere, C.; Kirk, M. L.; Wieghardt, K.; Girerd, J. J.; Solomon, E. I. *Inorg. Chem.* **1996**, *35*, 4323–4335.
(15) Williams, R. D.; Petrov, V. I.; Lu, H. P.; Hupp, J. T. *J. Phys. Chem. A* **1997**, *101*, 8070–8076.
(16) Brunschwig, B. S.; Creutz, C.; Sutin, N. *Chem. Soc. Rev.* **2002**, *31*, 168–184.
(17) Sun, H.; Steeb, J.; Kaifer, A. E. *J. Am. Chem. Soc.* **2006**, *128*, 2820–2821.
(18) Concepcion, J. J.; Dattelbaum, D. M.; Meyer, T. J.; Rocha, R. C. *Philos. Trans. R. Soc. London, Ser. A* **2008**, *366*, 163–175.
(19) Osella, D.; Gobetto, R.; Nervi, C.; Ravera, M.; D'Amato, R.; Russo, M. V. *Inorg. Chem. Commun.* **1998**, *1*, 239–245.
(20) Burgess, M. R.; Jing, S.; Morley, C. P. *J. Organomet. Chem.* **2006**, *691*, 3484–3489.
(21) Wedeking, K.; Mu, Z. C.; Kehr, G.; Sierra, J. C.; Lichtenfeld, C. M.; Grimme, S.; Erker, G.; Frohlich, R.; Chi, L. F.; Wang, W. C.; Zhong, D. Y.; Fuchs, H. *Chem.—Eur. J.* **2006**, *12*, 1618–1628.
(22) Ferguson, G.; Glidewell, C.; Opromolla, G.; Zakaria, C. M.; Zanello, P. *J. Organomet. Chem.* **1996**, *517*, 183–190.
(23) Arisandy, C.; Fullam, E.; Barlow, S. *J. Organomet. Chem.* **2006**, *691*, 3285–3292.
(24) Morrison, W. H.; Krogsrud, S.; Hendrick, D. N. *Inorg. Chem.* **1973**, *12*, 1998–2004.
(25) Chen, W.; Chen, S. W.; Ding, F. Z.; Wang, H. B.; Brown, L. E.; Konopelski, J. P. *J. Am. Chem. Soc.* **2008**, *130*, 12156–12162.
(26) Chen, W.; Brown, L. E.; Konopelski, J. P.; Chen, S. W. *Chem. Phys. Lett.* **2009**, *471*, 283–285.
(27) Nishihara, H. *Bull. Chem. Soc. Jpn.* **2001**, *74*, 19–29.
(28) Dederichs, P. H.; Blugel, S.; Zeller, R.; Akai, H. *Phys. Rev. Lett.* **1984**, *53*, 2512–2515.
(29) Wu, Q.; Van Voorhis, T. *Phys. Rev. A* **2005**, *72*, 024502.
(30) Wu, Q.; Van Voorhis, T. *J. Chem. Theory Comput.* **2006**, *2*, 765–774.
(31) Behler, J.; Delley, B.; Lorenz, S.; Reuter, K.; Scheffler, M. *Phys. Rev. Lett.* **2005**, *94*, 036104–1.
(32) Behler, J.; Delley, B.; Reuter, K.; Scheffler, M. *Phys. Rev. B* **2007**, *75*, 115409–1.
(33) Schmidt, J. R.; Shenvi, N.; Tully, J. C. *J. Chem. Phys.* **2008**, *129*, 114110–1.
(34) Oberhofer, H.; Blumberger, J. *J. Chem. Phys.* **2009**, *131*, 064101–1.
(35) Wu, Q.; Van Voorhis, T. *J. Chem. Phys.* **2006**, *125*, 164105.
(36) Lowdin, P. O. *J. Chem. Phys.* **1950**, *18*, 365–375.
(37) Mayer, I. *Int. J. Quantum Chem.* **2002**, *90*, 63–65.
(38) Frisch, M. J.; Trucks, G. W.; Schlegel, H. B.; Scuseria, G. E.; Robb, M. A.; Cheeseman, J. R.; Montgomery, J. A., Jr.; Vreven, T.; Kudin, K. N.; Burant, J. C.; Millam, J. M.; Iyengar, S. S.; Tomasi, J.; Barone, V.; Mennucci, B.; Cossi, M.; Scalmani, G.; Rega, N.; Petersson, G. A.; Nakatsuji, H.; Hada, M.; Ehara, M.; Toyota, K.; Fukuda, R.; Hasegawa, J.; Ishida, M.; Nakajima, T.; Honda, Y.; Kitao, O.; Nakai, H.; Klene, M.; Li, X.; Knox, J. E.; Hratchian, H. P.; Cross, J. B.; Bakken, V.; Adamo, C.; Jaramillo, J.; Gomperts, R.; Stratmann, R. E.; Yazyev, O.; Austin, A. J.; Cammi, R.; Pomelli, C.; Ochterski, J. W.; Ayala, P. Y.; Morokuma, K.; Voth, G. A.; Salvador, P.; Dannenberg, J. J.; Zakrzewski, V. G.; Dapprich, S.; Daniels, A. D.; Strain, M. C.; Farkas, O.; Malick, D. K.; Rabuck, A. D.; Raghavachari, K.; Foresman, J. B.; Ortiz, J. V.; Cui, Q.; Baboul, A. G.; Clifford, S.; Cioslowski, J.; Stefanov, B. B.; Liu, G.; Liashenko, A.; Piskorz, P.; Komaromi, I.; Martin, R. L.; Fox, D. J.; Keith, T.; Al-Laham, M. A.; Peng, C. Y.; Nanayakkara, A.; Challacombe, M.; Gill, P. M. W.; Johnson, B.; Chen, W.; Wong, M. W.; Gonzalez, C.; Pople, J. A. *Gaussian 03*; Gaussian, Inc.: Wallingford, CT, 2004.
(39) Bylaska, E. J.; de Jong, W. A.; Kowalski, K.; Straatsma, T. P.; Valiev, M.; Wang, D.; Aprà, E.; Windus, T. L.; Hirata, S.; Hackler, M. T.; Zhao, Y.; Fan, P.-D.; Harrison, R. J.; Dupuis, M.; Smith, D. M. A.; Nieplocha, J.; Tipparaju, V.; Krishnan, M.; Auer, A. A.; Nooijen, M.; Brown, E.; Cisneros, G.; Fann, G. I.; Früchtl, H.; Garza, J.; Hirao, K.; Kendall, R.; Nichols, J.; Tsemekhman, K.; Wolinski, K.; Anchell, J.; Bernholdt, D.; Borowski, P.; Clark, T.; Clerc, D.; Dachsel, H.; Deegan, M.; Dyall, K.; Elwood, D.; Glendening, E.; Gutowski, M.; Hess, A.; Jaffe, J.; Johnson, B.; Ju, J.; Kobayashi, R.; Kutteh, R.; Lin, Z.; Littlefield, R.; Long, X.; Meng, B.; Nakajima, T.; Niu, S.; Rosing, M.; Sandrone, G.; Stave, M.; Taylor, H.; Thomas, G.; van Lenthe, J.; Wong, A.; Zhang, Z. *NWCHEM*; Pacific Northwest National Laboratory: Richland, WA, 2006.
(40) Becke, A. D. *J. Chem. Phys.* **1993**, *98*, 5648–5652.
(41) Lee, C. T.; Yang, W. T.; Parr, R. G. *Phys. Rev. B* **1988**, *37*, 785–789.
(42) Hay, P. J.; Wadt, W. R. *J. Chem. Phys.* **1985**, *82*, 270–283.
(43) Francl, M. M.; Pietro, W. J.; Hehre, W. J.; Binkley, J. S.; Gordon, M. S.; Defrees, D. J.; Pople, J. A. *J. Chem. Phys.* **1982**, *77*, 3654–3665.
(44) Klamt, A.; Schuurmann, G. *J. Chem. Soc., Perkin Trans. 2* **1993**, 799–805.
(45) McConnell, H. *J. Chem. Phys.* **1961**, *35*, 508–515.
(46) Powers, M. J.; Meyer, T. J. *J. Am. Chem. Soc.* **1978**, *100*, 4393–4398.
(47) Bildstein, B.; Denifl, P.; Wurst, K.; Andre, M.; Baumgarten, M.; Friedrich, J.; Ellmerermuller, E. *Organometallics* **1995**, *14*, 4334–4342.
(48) McAdam, C. J.; Brunton, J. J.; Robinson, B. H.; Simpson, J. *J. Chem. Soc., Dalton Trans.* **1999**, 2487–2495.
(49) Adams, R. D.; Qu, B.; Smith, M. D. *Organometallics* **2002**, *21*, 3867–3872.
(50) Rodriguez-Monge, L.; Larsson, S. *J. Phys. Chem.* **1996**, *100*, 6298–6303.
(51) Paddon-Row, M. N.; Wong, S. S. *Chem. Phys. Lett.* **1990**, *167*, 432–438.
(52) Farazdel, A.; Dupuis, M.; Clementi, E.; Aviram, A. *J. Am. Chem. Soc.* **1990**, *112*, 4206–4214.
(53) Sun, Q.; Bu, Y. X.; Qin, M. *J. Phys. Chem. A* **2003**, *107*, 1584–1596.

JP912049P